공학석사 학위논문

Catalytic oxidation of methane under non-thermal plasma condition

저온 플라즈마 조건에서 촉매에 의한 메탄의 산화반응

2014년 2월

서울대학교 대학원

화학생물공학부

이 희 수

Catalytic oxidation of methane under non-thermal plasma condition

지도교수 김도희

이 논문을 공학석사학위논문으로 제출함

2013년 12월

서울대학교 대학원

화학생물공학부

이 희 수

이희수의 석사학위논문을 인준함

2014년 2월

위 원 장 _____ (인)

부위원장 _____ (인)

위 원 _____ (인)

Abstract

Catalytic oxidation of methane under non-thermal plasma condition

Hee-su Lee
School of Chemical and Biological Engineering
The Graduate School
Seoul National University

As one of greenhouse gases, methane is recognized to contribute to the major portion of global warming. The stable C-H bond in methane requires the large amount of noble metal catalyst to be oxidized completely at low temperature (i.e. below 500℃). Thus, we aim at lowering the light-off temperature by introducing the plasma-catalyst hybrid reaction system. The catalytic reaction needs activation energy to induce the reaction, so the motivation of this research is that the plasma is able to help reduce the activation energy by synthesizing the active radicals. There are two types of plasma

source, one is thermal plasma and the other is non-thermal plasma. The thermal plasma had a possibility to interrupt the examination of plasma-catalyst hybrid interaction by increasing the catalyst bed temperature, thus the non-thermal plasma, especially the dielectric barrier discharge(DBD) was used in this research. In this experiment, the complete oxidation of methane was carried out in a DBD quartz tube reactor. Catalyst and plasma were hybridized into one in-plasma catalysis system. The palladium-based catalysts such as Pd/Al_2O_3, Pd/CeO_2, $Pd/Ce_{0.7}Zr_{0.3}O_2$, Pd/SiO_2, and Pd/TiO_2 were used as oxidation catalyst because palladium-based catalysts have shown the greatest oxidative ability of methane so far. In order to separate the catalytic effect from the plasma one, methane oxidation was evaluated over the catalyst in the presence or in the absence of plasma at the fixed plasma operating conditions including waveform, and frequency. Though, input voltage of the plasma-catalyst reactor varied from $2kV_{p-p}$ to $5kV_{p-p}$ to observe which input voltage offered the best circumstance for plasma-catalyst interaction. Also, to measure plasma effect, plasma power was calculated by V-Q Lissajous figure method. In the absence of catalyst, the methane was started to decompose from room temperature, and the conversion increased with the increment of temperature since dielectric constant of dielectric(quartz tube reactor) were changed along the temperature. In these reactions, not only CO_2 but CO was also produced. As the input voltage increased from $2kV_{p-p}$ to $4kV_{p-p}$, the methane conversion also increased sharply because

of the upsurge of specific input energy. In the presence of catalyst alone, methane started to be activated above 200℃ for all the cases. However, in the presence of both plasma and catalyst, methane was oxidized at room temperature and the selectivity of CO which should not be produced was retained at zero percent. These results cannot be achieved in the cases of both catalyst only reaction and plasma only reaction. As the input voltage went higher, the plasma influence got stronger, so the catalytic performance was hardly observable. At low input voltage like $2kV_{p-p}$, all plasma-catalyst hybrid reaction did not shift the reaction-end temperature, but showed the activation of methane at room temperature and catalytic performances while they disappeared at higher input voltage. Also, Pd/Al_2O_3 presented slightly higher methane conversion than plasma only reaction at all input voltage conditions. In terms of energy efficiency, it was shown that using relatively low specific input energy could enhance the methane oxidation conversion even at ambient temperature. In summary, it was found that non-thermal plasma played an important role in converting methane to CO/CO_2 in the temperature range where catalyst hardly worked, thus leading to facilitate methane oxidation with catalyst at lower temperature.

Keywords : Methane oxidation, catalyst-plasma hybrid reaction, palladium, dielectric barrier discharge

Student number : 2012-20970

Contents

List of Figures

List of Tables

Chapter 1. Introduction

1.1 Necessity of methane complete oxidation

The world-wide presence of natural gas, much larger than crude oil and the fact that natural gas is clean energy source compared to other fossil fuels make it an attractive alternative energy source. Nowadays, it is used as a fuel of combined heat power(CHP) and public transportation such as bus and natural gas vehicles(NGV) [1]. Recently, it has become more attractive energy source since the new method of shale gas(natural gas) production was discovered in many countries like USA, China, Mexico, Argentina, Poland, etc [2]. Despite of these advantages, the emission of unburned natural gas because of its stable structure makes it difficult to use since the methane, which was the main component of natural gas, is recognized as the major portion of global warming and led to dissipation of energy. It contributes more to global warming than carbon dioxide at equivalent emission rate and has quite long lifetime. As shown in table 1, after Euro Ⅲ, regulations for the use of NGVs in urban areas, especially heavy-duty vehicles, are currently being developed rapidly in most industrial countries [1]. In this way, complete oxidation of methane is one of the critical topics in environmental and energy efficiency control.

Table 1 European heavy-duty diesel and gas emission limit values (g/kWh) [1]

Tier	Implementation	Test cycle	CO	THC	NMHC	NO_x	Particulate matter	Smoke (m^{-1})
Euro Ⅱ		ECE R-49	4.0	1.1	-	7.0	0.15	
Euro Ⅲ[b]	October 2000	ESC/ELR	2.1	0.66	-	5.0	0.10	0.8
		ETC	5.45	1.6[a]	0.78	5.0	0.16	
Euro Ⅲ EEV[c]	October 1999	ESC/ELR	1.5	0.25	-	2.0	0.02	0.15
		ETC	3.0	0.65[a]	0.4	2.0	0.02	
Euro Ⅳ	October 2005	ESC/ELR	1.5	0.46	-	3.5	0.02	0.5
		ETC	4.0	1.1[a]	0.55	3.5	0.03	
Euro Ⅴ	October 2008	ESC/ELR	1.5	0.46	-	2.0	0.02	0.5
		ETC	4.0	1.1[a]	0.55	2.0	0.03	

$1\text{kWh} = 3.6 \times 10^6\text{J}$.

[a] CH_4 for natural gas engine only.

[b] Directive 1999/96/EC of 13 December 1999.

[c] A special low-emission vehicle class (environmentally enhanced vehicle, EEV) is defined. Tax incentives can be granted for vehicles complying with theses requirements.

1.2 Concept of plasma

Many studies have been performed to design methane complete oxidation catalysts such as palladium-based catalysts [3-6], platinum-based catalysts [6] which were less used than palladium-based catalysts, and non-noble metal catalysts such as mixed oxide catalysts [7-11]. Though, it was difficult to achieve proper reaction temperature(below 200℃) compared to other exhaust gas like NOx or CO. An alternative way to catalytic oxidation of methane can be the use of plasma. Plasma is a partially or fully ionized gas phase consisting of various particles, such as electrons, ions, atoms, and molecules [12]. There are various thermal and non-thermal plasma sources such as dielectric barrier discharge (DBD), corona, gliding arc, rotating arc, spark, microwave, glow discharge and pulsed discharge with catalyst or without catalyst [13, 14]. Plasma can be divided into two types in terms of plasma temperature: electron temperature and gas temperature [15]. The former is non-thermal plasma and the latter is thermal plasma. Thermal plasma is in a phase where almost all components are at thermal equilibrium. Its example is arc plasma, in which high-temperature(>10,000K) thermal energy needs to decompose hydrocarbons or complex materials into basic elements such as hydrogen or carbon monoxide. On the other hand, the energy input to generate non-thermal plasma is very small and the temperature increase of the inlet gas and the reactor is

relatively small compared with thermal plasma. In some cases, the temperature increased by non-thermal plasma is only few degrees [16]. In the non-thermal plasma, high-energy electrons (1-20eV) are produced and activate other various radicals, thus temperature is not in thermal equilibrium and the temperature quite differs between the electrons and the other particles like ions, atoms, and molecules. Thus, gas temperature can be maintained at low degree since electron mass is very light. In this sense, non-thermal plasma is also referred to as "cold plasma" or "nonequilibrium plasma" [12]. Partially ionized gas, in which the gas temperature maintains near room temperature, can be created using simple configuration and relatively inexpensive power source.

1.3 Dielectric barrier discharge (DBD) plasma

Various plasma sources are currently used for environmental problems. Among those, DBD which requires alternating voltage and at least one dielectric barrier between high voltage electrode and ground electrode [17] was used in this experiment because of its significant benefits. First of all, non-thermal plasma like DBD is easy to generate. DBD hardly converts to unstable spark or arc because of the existence of a dielectric barrier gap [13]. Second, DBD has long and proven history since its investigation in 1857. Its physical and chemical properties and industrial applications are well developed [17]. Third, DBD can form various electrode and reactor configurations such as micro-reactors, gas to liquid interface, fluidized beds [13]. Lastly, DBD reactor can be manufactured using inexpensive materials like glass or polymer. Thus, DBD itself is in widespread use for industrial application such as water and air treatment, CO_2 lasers, excimer lamps, plasma display panels [18]. The dielectric in DBD conducts some functions. First, it cuts the current flow through the discharge gap after a few nanoseconds. Then, the resulting microdischarges in the discharge gap are distributed uniformly over the whole electrode area. Because of the dielectric barrier, the DBD is a non-equilibrium discharge, which means high temperature electrons are created in the microdischarges. They can cause plasma chemical reactions, but the temperature of

heavier particles such as molecules, ions, atoms retain near the average gas temperature in the discharge gap, so the total gas or reactor temperature can be maintained near the ambient temperature. When the specific input energy density in DBD reactor is reduced to values below 100 J/L gas heating effects get less important. Moreover, a specific input energy density of 10 J/L can increase the gas temperature of 10−15℃ which is low in terms of plasma temperature depending on the gas mixture [19].

1.4 Plasma-catalyst hybrid system

Plasma and catalyst have their own advantages and disadvantages. The catalyst is highly selective, but active only at high temperature since reactants overcome the activation energy while plasma becomes reactive even at room temperature, but is nonselective. Hence, hybridization of plasma and catalyst into one system can provide complementary or even synergistic results via presenting a solution for the low-temperature activation of a catalyst [20], and past studies have shown the positive effect of using a plasma-catalyst combination system in a diverse formation [21-25]. Heterogeneous catalyst can be combined with non-thermal plasma in two way: by introducing the catalyst in the discharge zone (in-plasma catalysis, IPC) or by placing the catalyst after the discharge zone (post plasma catalysis, PPC) as shown below in Fig. 1. Heterogeneous catalyst can be put into a reactor in several ways as a packed bed, a layer of catalyst material or coating on the reactor wall or electrodes [26]. In order to obtain an influence of radical formation on catalytic reactions the radical formation has to take place near the catalyst surface. In this concept, in-plasma catalysis was used in this paper. In this research, methane complete oxidation (combustion) reactions using DBD plasma reactor with palladium-based catalysts in the presence of plasma and in the

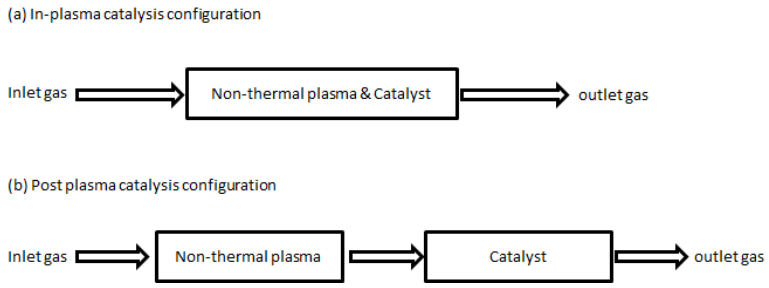

Fig. 1. Schematic overview of two plasma-catalyst hybrid system configurations; (a) in-plasma configuration (IPC) and (b) post plasma configuration (PPC).

absence of plasma were investigated. Reaction tests were conducted in a simple noble gas condition to examine the hybridization effect of plasma and oxidation catalyst.

Chapter 2. Experimental

2.1 Preparation of catalyst

In this experiment, commercial supports ($\gamma-Al_2O_3$, SiO_2, TiO_2, $Ce_{0.7}Zr_{0.3}O_2$, CeO_2) were used. These powder supports were calcined at 500℃ for 5h in air. Palladium supported catalysts were synthesized by incipient wetness impregnation method. The solution of $Pd(NO_3)_2 \cdot 2H_2O$ precursor obtained from Sigma Aldrich was added into the supports. The loading amount of palladium in its metallic state was 2wt.% of the catalysts. The catalysts were dried and subsequently calcined in air (N_2:O_2=85:15) at 773K for 2h. The catalysts particle size were fixed to 425-600 ㎛. The identification of solid-state phases by X-ray diffraction (XRD) was performed on a RIGAKU run at 40kV, 50mA. Specific surface area of catalysts was determined by the BET method using ASAP 2010 nitrogen adsorption. The catalysts in bead form (Φ=425-600 ㎛) were placed at the middle of reactor, just above the filter, inside the discharge zone. The height of catalyst bed varied from 5mm to 15mm since the weight of catalyst was maintained at 0.5g while the density of them differed from each other. The catalyst bed temperature was measured using two K type thermocouples. One was affixed to the outer reactor surface and the other which was protected by another quartz tube was located just

below the filter. In this paper, temperature data measured at the thermocouple placed in the reactor was used.

2.2 Plasma-catalysis system

A schematic view of plasma-catalysis system is presented in Fig. 2. Fig. 2 shows the experimental apparatus, consisting of a 1000:1 high voltage probe (Tektronics P6015A), a current probe (Pearson electronics 6585), and a capacitor(1000 pF) for measuring voltage (V), current (A), and transferred electric charge (Q), respectively. All output signals were transmitted to a 100MHz digital oscilloscope (Tektronics DPO 2014) that measures discharge power using the V-Q Lissajous figure method [27, 28].

The DBD reactor was a quartz tube with an inner diameter of 10mm a thickness of 1.3mm and a length of 500mm. The filter was located at the middle of reactor and its thickness was 2.5mm. Configuration of this reactor is indicated in Fig. 3. In this reactor, catalyst zone and plasma zone were combined at same position. Electrical discharge of the reactor was DBD. It consisted of a SUS rod of which thickness was 3mm. The rod was centered in a quartz tube reactor, fixed with a groove at the filter and teflon ferrule. The outer surface of the reactor was surrounded by SUS plate with a length of 20mm and a thickness of 0.8mm. The length of discharge zone was 200mm, and the gap was 5mm, resulting in a reaction volume of about 2.5cm^3. To create the discharge an AC high voltage was generated with a maximum of 5kV_{p-p}. The AC high voltage was supplied by TREK 20/20C-HS with a maximum peak voltage of

20kV and a variable frequency up to 20kHz. All experiments were carried out under identical conditions of driving frequency (4kHz) with the amplitude of the applied voltage varied between $2kV_{p-p}$ and $5kV_{p-p}$ in internal of 1kV.

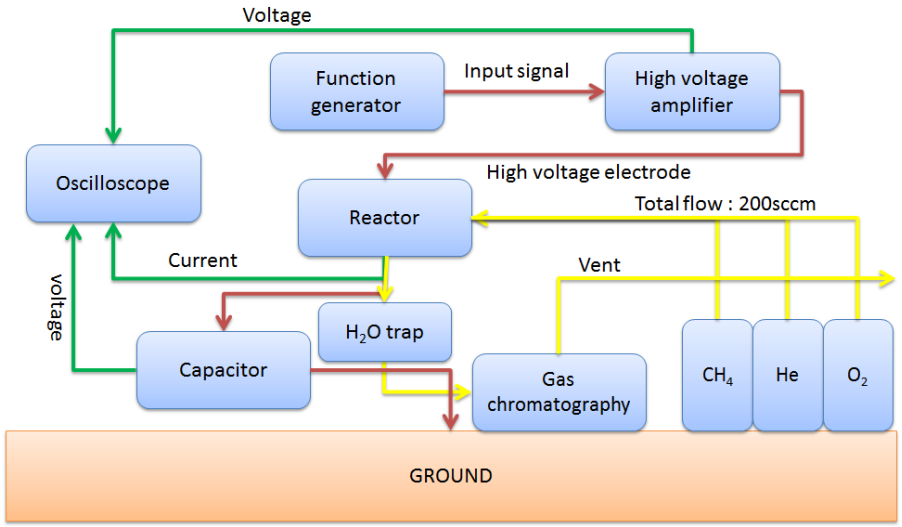

Fig. 2. Schematic view of plasma-catalysis system.

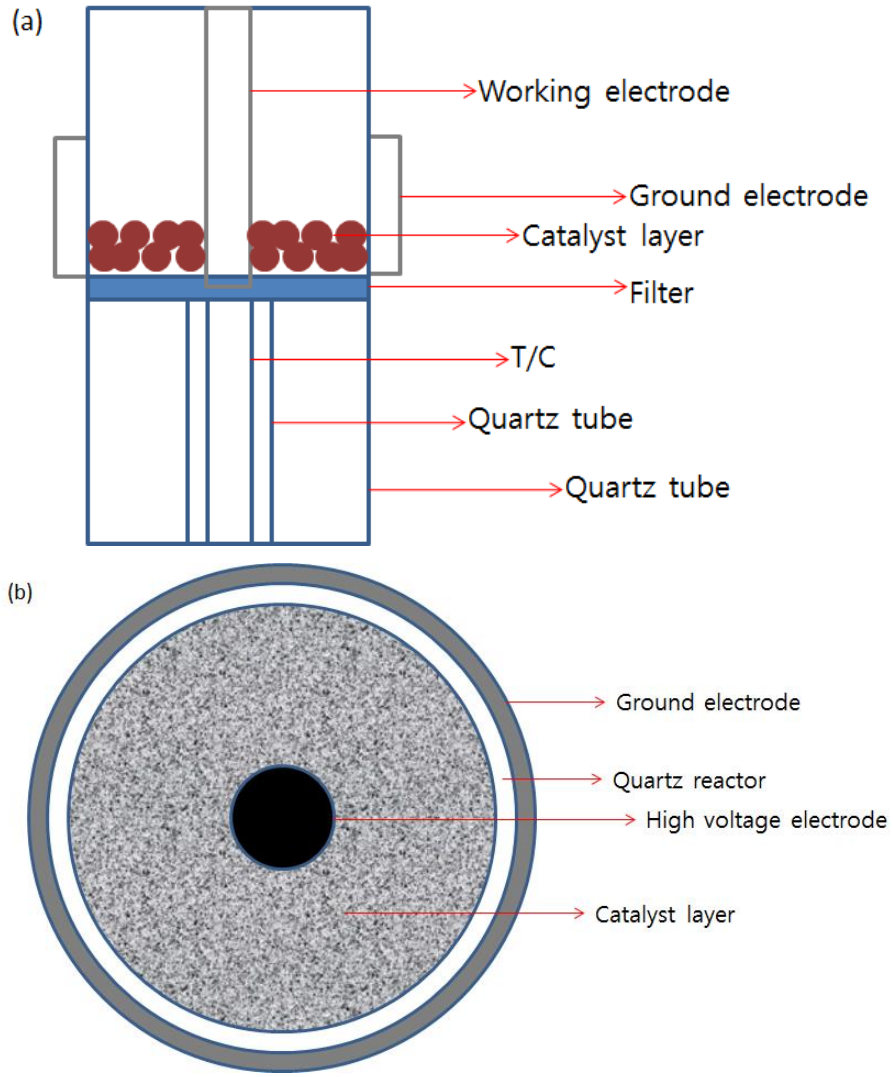

Fig. 3. Configuration of quartz reactor; (a) horizontal view of the reactor. (b) vertical view of the reactor.

2.3 Lissajous method

According to the gas discharge theory, the DBD plasma can be equal to the charge and discharge transitions of the capacitor [27, 29]. The capacitor was placed between the ground electrode of the reactor and the ground to examine the transported charges. Expected Lissajous figure [27] and related equations are followed in Fig. 4 and Eqs. (1−3). According to the equations, the plasma power can be obtained by measuring the area of the V−Q Lissajous cyclogram. In Fig. 4, the lines A−B and C−D represent the discharge transitions. The slope of them is equal to dielectric capacitance. The lines B−C and A−D represent the capacitive transitions. Their slope is equal to the total capacitance of the discharge reactor [27].

$$P = \frac{1}{T}\int_0^T U(t)I(t)dt \tag{1}$$

$$P = \frac{1}{T}\oint U(Q)dQ = C_M f \oint U(U_C)dU_C = f \cdot S \tag{2}$$

$$\text{Specific input energy(J)} = \frac{\text{discharge power(W)}}{\text{gas flow rate}\left(\frac{1}{s}\right)} \tag{3}$$

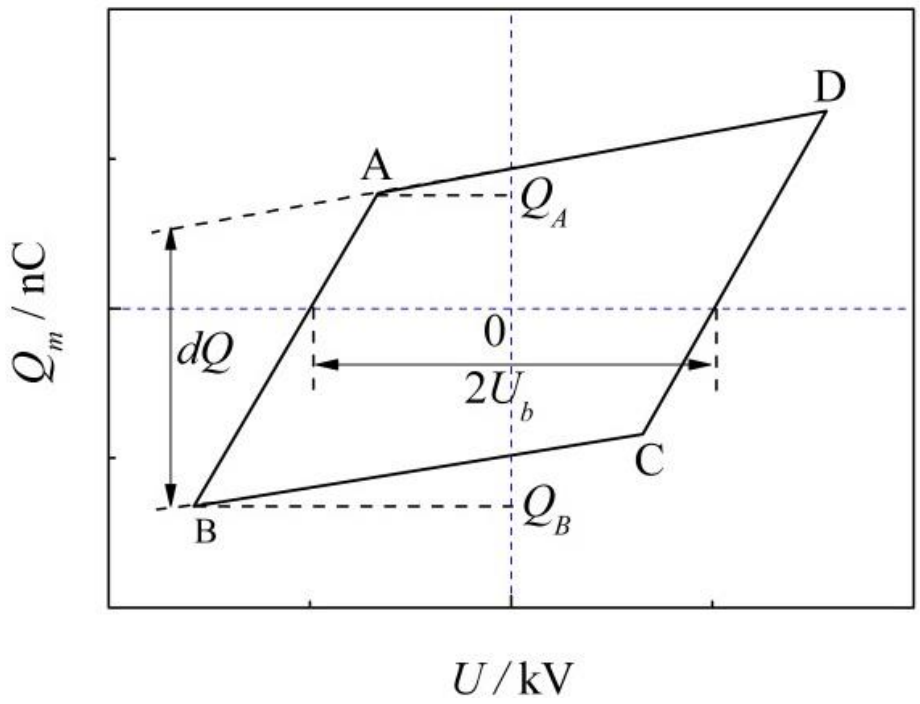

Fig. 4. Ideal Lissajous figure [27].

2.4 Analytic condition

The catalytic activity was measured at atmospheric pressure in the same plasma quartz reactor. The reactants are the following: 2.5% O_2, 2500 ppm CH_4 in He as noble gas balance to simplify the reaction mechanism. The O_2 mixture contained 10% O_2, 90% He. The CH_4 mixture contained 1% CH_4, 99% He. The total gas flow was maintained at 200sccm. Each of gas mixture was metered by using calibrated electronic mass flow controllers. Outflow gases passing through the discharge region were analyzed by gas chromatography (AGILENT GC 6890N) equipped with a thermal conductivity detector (TCD) and a 60/80 Carboxen-1000 packed column with temperature programming from 35℃ to 225℃. Methane conversion at steady-state was examined in the presence and in the absence of catalyst at different temperatures, ranging from room temperature to about 400℃. Methane conversion and selectivity of the CH_4, CO, and CO_2 species are defined in Eqs. (4-6):

$$\text{Conversion}\ (CH_4) = \frac{mole\ (consumed\ CH_4)}{mole\ (introduced\ CH_4)} \times 100\ [\%] \quad (4)$$

$$\text{Selectivity}\ (\text{CO}) = \frac{mole\ (produced\ CO)}{mole\ (converted\ CH_4)} \times 100\ [\%] \quad (5)$$

$$\text{Selectivity}\ (CO_2) = \frac{mole\ (produced\ CO_2)}{mole\ (converted\ CH_4)} \times 100\ [\%] \quad (6)$$

Chapter 3. Results and discussion

3.1 Effect of input energy

One set of experiments has been carried out without catalyst first to compare with the reaction involving both plasma and catalyst. The methane conversion, the CO concentration, and the CO/CO_2 ratio results were followed as function of temperature and as function of energy deposition. It is well known that plasma input power is one of the important parameters in DBD plasma–catalysis reaction [19, 30, 31]. The specific input energy was measured by Lissajous figure method and the sample Lissajous figure is presented in Fig. 5. In the same input voltage and frequency, the plasma power varied slightly with the temperature because the dielectric constant of dielectric (quartz reactor) was changed with the temperature. In this concept, the specific input energy ranged from 12 to 26 J/L at $2kV_{p-p}$ as input voltage, from 37 to 55 J/L at $3kV_{p-p}$ as input voltage, from 100 to 161 J/L at $4kV_{p-p}$ as input voltage, and from 222 to 269 J/L at $5kV_{p-p}$ as input voltage. The effect of the specific input energy on methane conversion as function

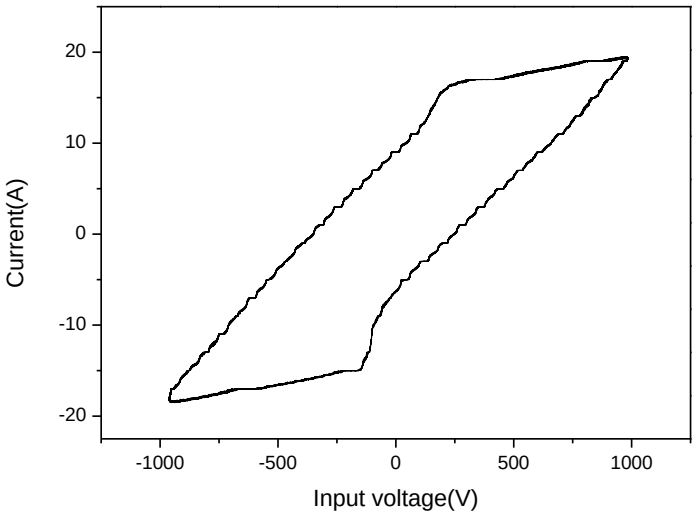

Fig. 5. Lissajous figure at $2kV_{p-p}$ input voltage in the absence of catalyst.

of temperature is presented in Fig. 6. Table 2 also indicates that the conversion of methane increases with the temperature and specific input energy. For all temperature range, the lower thermal energy was needed with increasing the energy deposition increasing. Since the electrical energy at $5kV_{p-p}$ reached quite high value and this caused energy inefficiency, the input voltage condition of $5kV_{p-p}$ was excluded. The CO concentration and the CO selectivity are indicated at Fig. 7. CO concentrations and selectivities went down as the temperature rose since the relatively reactive CO was oxidized to CO_2. In the case of $2kV_{p-p}$, CO selectivity was very high under the lower temperature. All results can be explained by more active species generated at higher specific input energy. Methane and oxygen were dissociated through energy rich plasma electrons to a methyl, hydrogen, and oxygen radicals [32]. Oxygen radicals were very reactive and abundant in this condition compared to methane, thus these oxygen radicals reacted with methyl or hydrogen radicals, which was resulted in CO, CO_2, and H_2O. The discharge voltage and current shaped are presented in Fig. 8. This figure shows that most of the discharge current existed at the point of inflection of the applied voltage, exhibiting a discharge current pattern with an active period of discharge was slightly shifted.

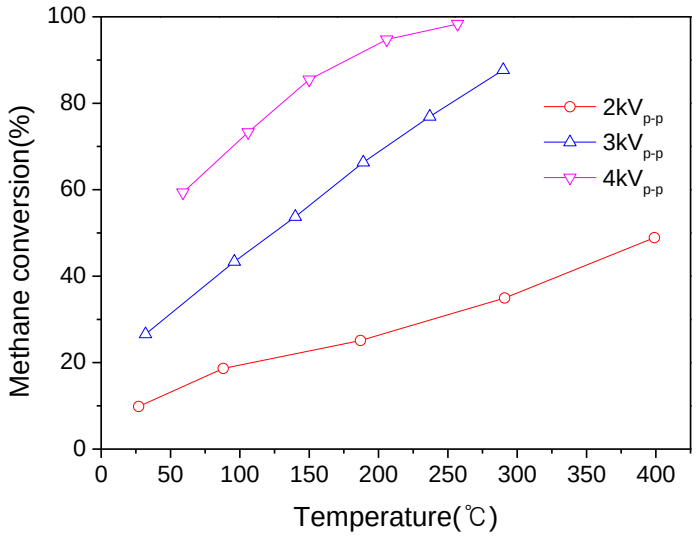

Fig. 6. Effect of temperature on the methane conversion in the absence of catalyst.

Table 2 Temperature required to earn n% methane conversion

Input voltage (specific input energy range)	Light-off temperature (℃)			
	T_{20}	T_{40}	T_{60}	T_{85}
2kV (12 - 26 J/L)	105	332	-	-
3kV (37 - 55 J/L)	-	83	164	277
4kV (100 - 161 J/L)	-	-	60	150
5kV (222 - 269 J/L)	-	-	-	100

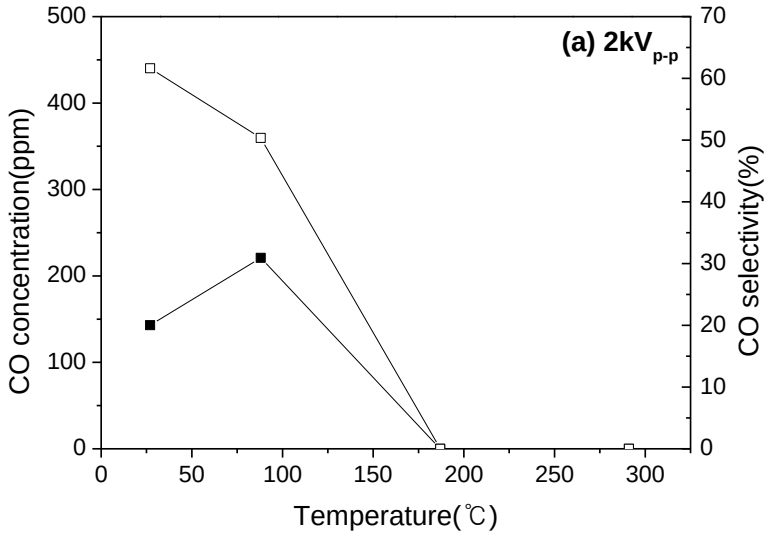
(a) 2kV$_{p-p}$
CO concentration(ppm)
CO selectivity(%)
Temperature(℃)
0
100
200
300
400
500
0
10
20
30
40
50
60
70
0
50
100
150
200
250
300

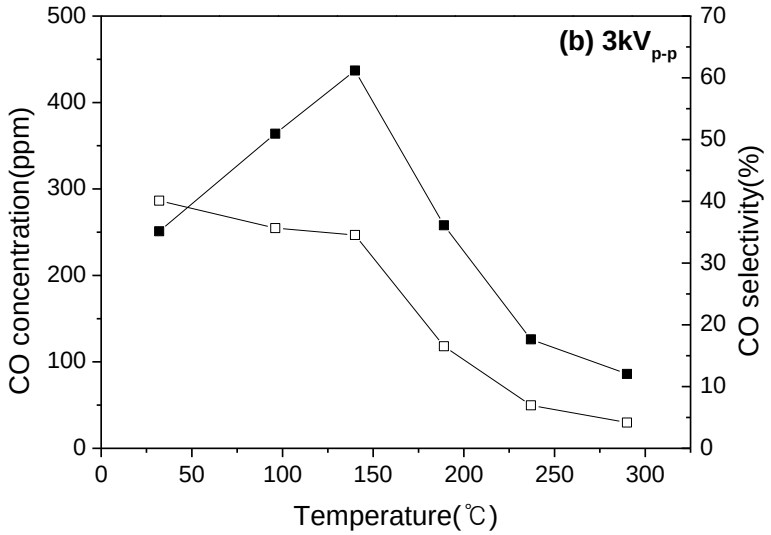
(b) 3kV$_{p-p}$
CO concentration(ppm)
CO selectivity(%)
Temperature(℃)
0
100
200
300
400
500
0
10
20
30
40
50
60
70
0
50
100
150
200
250
300

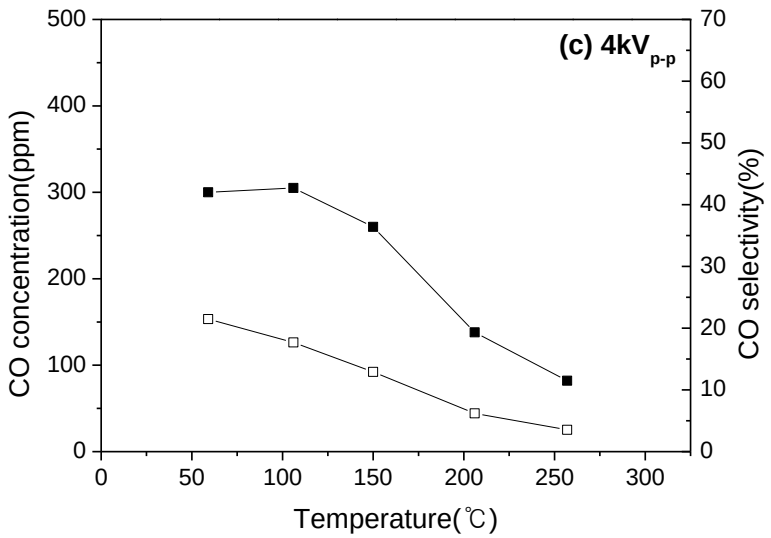

Fig. 7. Effect of temperature on the CO concentration(close symbols) and CO selectivity(open symbols) in the absence of catalyst. (a) Input voltage = 2kV$_{p-p}$. (b) Input voltage = 3kV$_{p-p}$. (c) Input voltage = 4kV$_{p-p}$

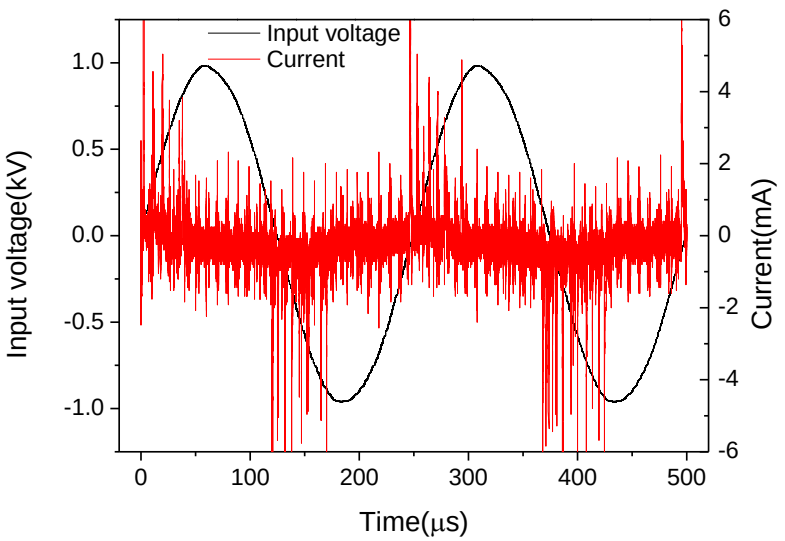

Fig. 8. Input voltage and subsequent current characteristics of the reactor at $2kV_{p-p}$, room temperature.

3.2 Catalytic performance

The specific surface area of the catalysts is shown in Table 3. According to the result, Pd/γ−Al_2O_3, Pd/SiO_2 had high surface area. The methane conversion as function of temperature over various Pd−based catalysts without plasma is presented in Fig. 9. Palladium loading amount of the catalysts was maintained at 2wt.%. In the absence of plasma, all catalysts were activated above 200℃, but Pd/TiO_2 had slightly lower activity compared to other catalysts. Pd/SiO_2 and Pd/$\gamma-Al_2O_3$ showed best performance on the methane combustion without plasma. The reactions were performed through complete oxidation since CO did not produced at all and all the product gases were CO_2. Table 4 also shows the catalytic performance of various Pd−based catalysts.

Table 3 Specific surface area of the catalysts

Catalyst	Specific surface area(m^2/g)
Pd/SiO_2	151
$Pd/Ce_{0.7}Zr_{0.3}O_2$	126
Pd/TiO_2	80
Pd/CeO_2	124
$Pd/\gamma-Al_2O_3$	240

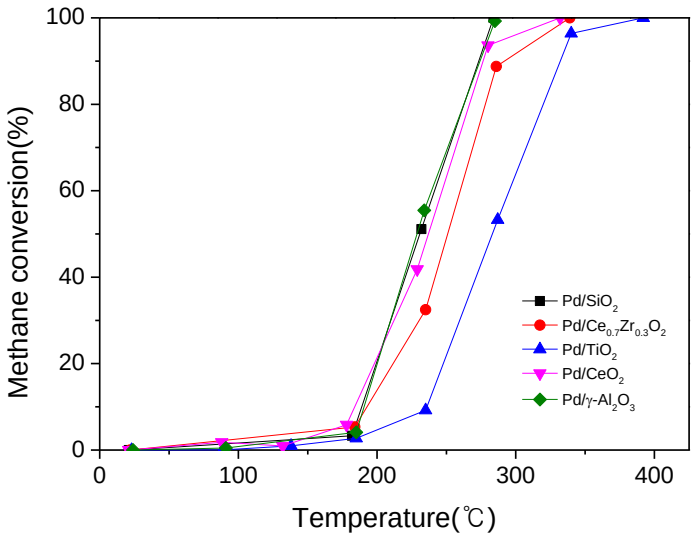

Fig. 9. Catalytic performance of Pd-based catalysts as a function of temperature without DBD plasma.

Table 4 Catalytic performance on the CH_4 conversion of various palladium-based catalysts

Catalyst	Light-off temperature (℃)		
	T_{10}	T_{50}	T_{90}
Pd/SiO_2	188	232	274
$Pd/Ce_{0.7}Zr_{0.3}O_2$	193	251	291
Pd/TiO_2	235	284	332
Pd/CeO_2	184	236	276
$Pd/\gamma-Al_2O_3$	191	228	274

3.3 Plasma catalytic oxidation of methane

After the measurement of catalytic performance of the catalysts, the catalysts were placed inside the discharge zone of plasma to investigate the effect of plasma-catalyst hybridization. This concept was based on other plasma-catalysis applications such as toluene decomposition [33, 34], methane reforming [18, 35-37] in which the studies that the combination of plasma and catalyst resulted in a better reactivity and selectivity than catalyst alone or plasma alone. Compared with each of catalytic performance, the plasma catalytic oxidation of methane reaction results under various palladium-based catalysts as functions of temperature and input voltage are shown in Fig. 10. In these figures, methane conversion of plasma-catalyst hybrid reaction exceeded those of catalyst only reaction at almost all cases. Moreover, even at room temperature, the oxidation reaction of methane started. In the case of $2kV_{p-p}$ and $3kV_{p-p}$, the slopes of the graphs were changed at the catalysts' light-off temperature. Though, the reactions terminated at similar temperature, which means the DBD plasma could not change the reaction-end temperature. As the input voltage increased, the influence of plasma grew rapidly while that of catalyst disappears. In Fig. 11, the methane conversion results of plasma-catalyst hybrid reaction compared with plasma only reaction are presented. Except the case of $Pd/\gamma-Al_2O_3$, the catalysts with DBD plasma had lower

(a)

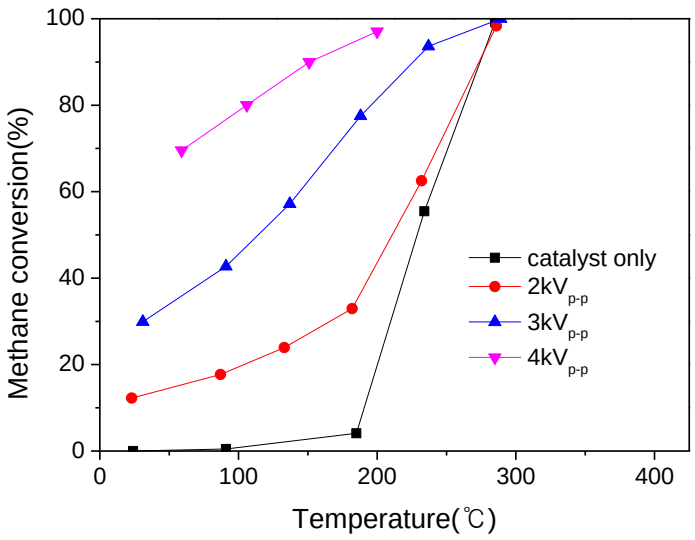
Methane conversion(%)
Temperature(℃)
catalyst only
2kV p-p
3kV p-p
4kV p-p

(b)

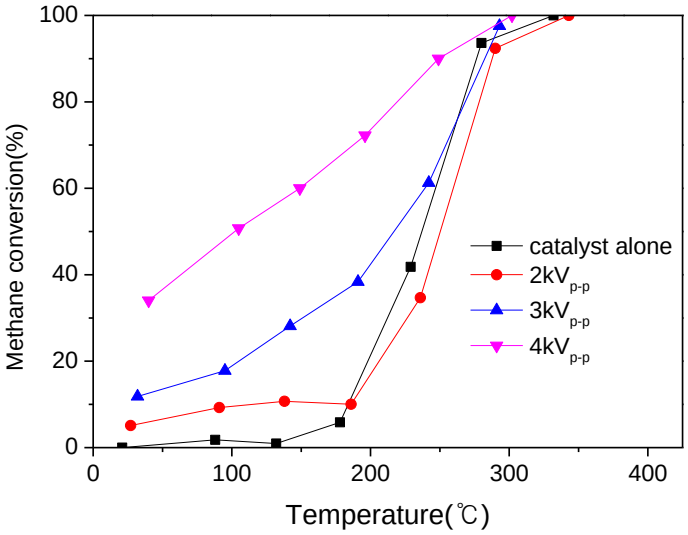
Methane conversion(%)
Temperature(℃)
catalyst alone
2kV p-p
3kV p-p
4kV p-p

(c)

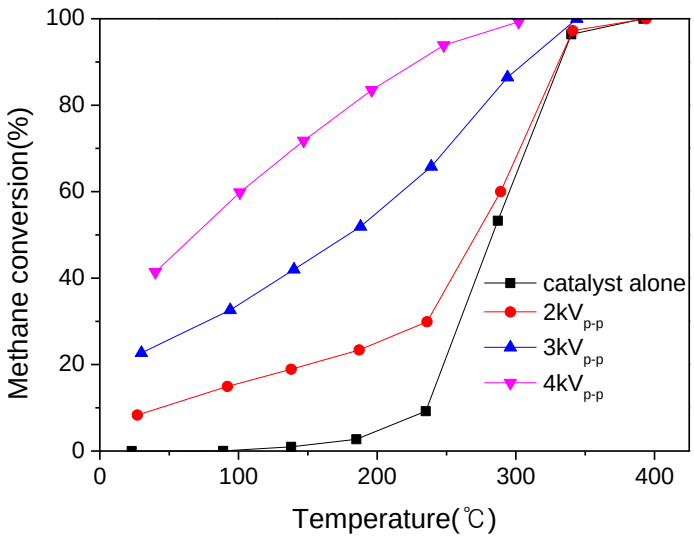
Methane conversion(%)
Temperature(℃)
catalyst alone
2kV p-p
3kV p-p
4kV p-p

(d)

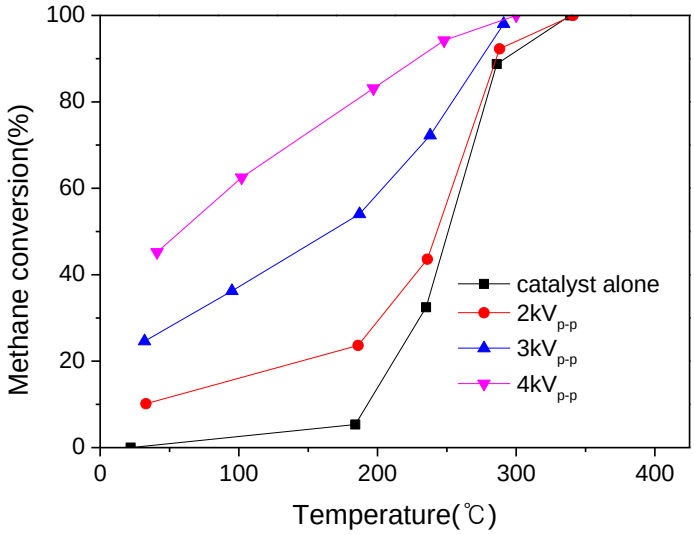
Methane conversion(%)
Temperature(℃)
catalyst alone
2kV p-p
3kV p-p
4kV p-p

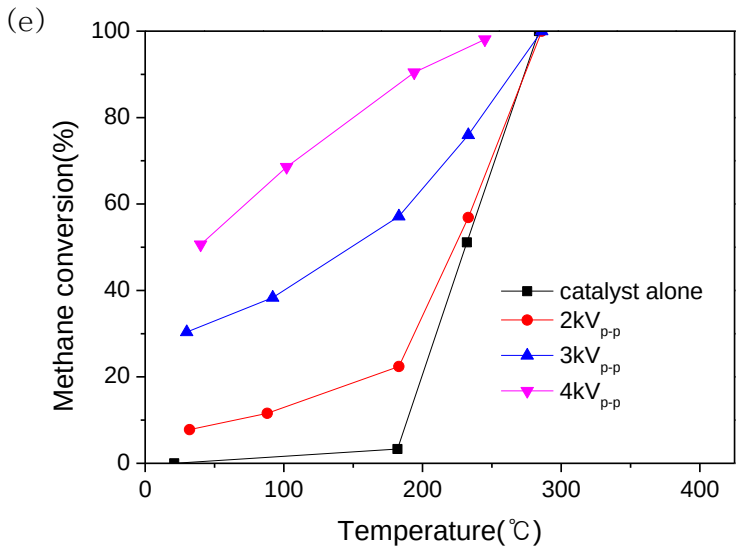

Fig. 10. Effect of temperature and input voltage on the methane conversion in the plasma-catalyst hybrid system compared with catalyst only reaction. (a) Pd/γ-Al_2O_3. (b) Pd/CeO_2. (c) Pd/TiO_2. (d) Pd/$Ce_{0.7}Zr_{0.3}O_2$. (e) Pd/SiO_2.

(a)

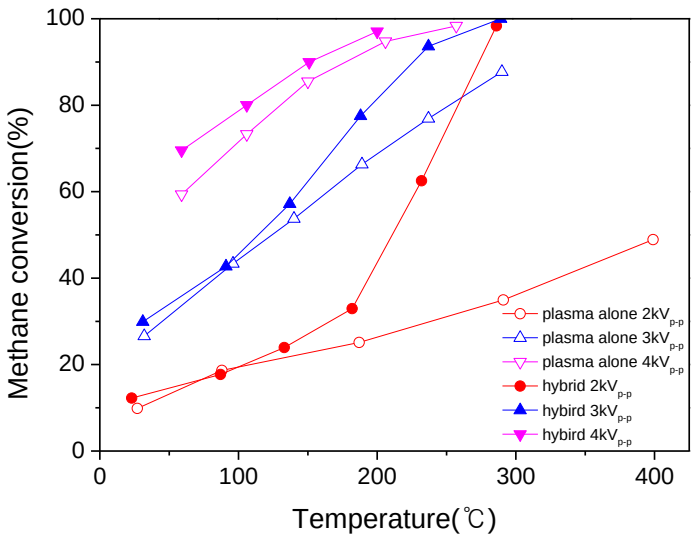
Methane conversion(%)
Temperature(℃)
0
20
40
60
80
100
0
100
200
300
400
plasma alone 2kV$_{p-p}$
plasma alone 3kV$_{p-p}$
plasma alone 4kV$_{p-p}$
hybrid 2kV$_{p-p}$
hybird 3kV$_{p-p}$
hybird 4kV$_{p-p}$

(b)

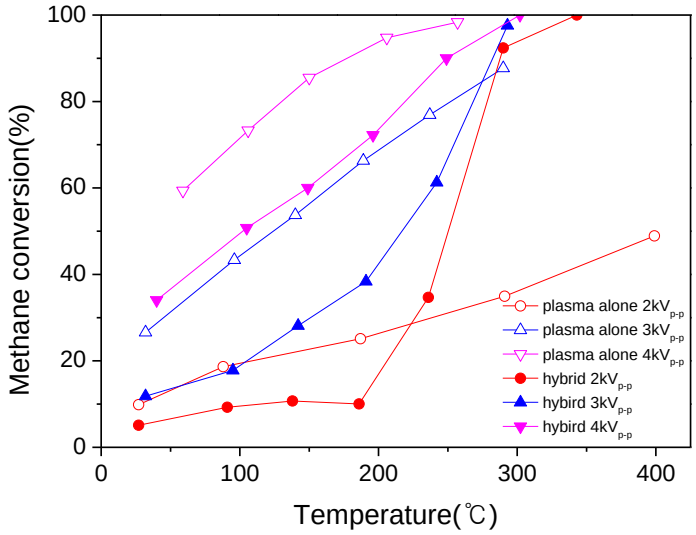
Methane conversion(%)
Temperature(℃)
0
20
40
60
80
100
0
100
200
300
400
plasma alone 2kV$_{p-p}$
plasma alone 3kV$_{p-p}$
plasma alone 4kV$_{p-p}$
hybrid 2kV$_{p-p}$
hybird 3kV$_{p-p}$
hybird 4kV$_{p-p}$

(c)

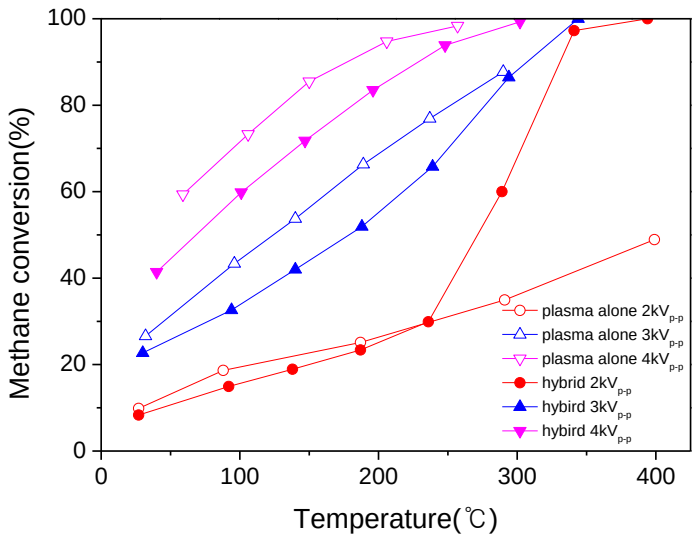
Methane conversion(%)
Temperature(℃)
0
20
40
60
80
100
0
100
200
300
400
plasma alone 2kV$_{p-p}$
plasma alone 3kV$_{p-p}$
plasma alone 4kV$_{p-p}$
hybrid 2kV$_{p-p}$
hybird 3kV$_{p-p}$
hybird 4kV$_{p-p}$

(d)

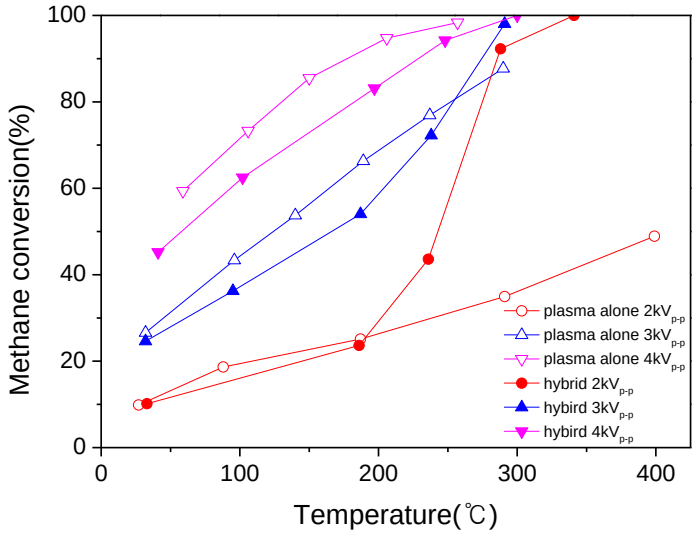
Methane conversion(%)
Temperature(℃)
0
20
40
60
80
100
0
100
200
300
400
plasma alone 2kV$_{p-p}$
plasma alone 3kV$_{p-p}$
plasma alone 4kV$_{p-p}$
hybrid 2kV$_{p-p}$
hybird 3kV$_{p-p}$
hybird 4kV$_{p-p}$

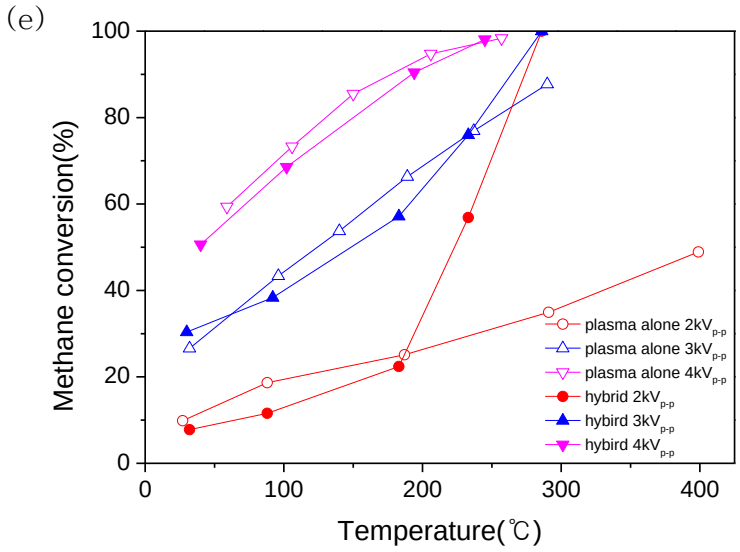

Fig. 11. Effect of temperature and input voltage on the methane conversion in the plasma-catalyst hybrid system compared with plasma only reaction. (a) Pd/γ-Al_2O_3. (b) Pd/CeO_2. (c) Pd/TiO_2. (d) Pd/$Ce_{0.7}Zr_{0.3}O_2$. (e) Pd/SiO_2.

activity than plasma only reaction which meant the catalysts underwent antagonistic effect when hybridized with plasma. However, in terms of CO selectivity which should be retained at zero percent in this experiment, plasma-catalyst hybrid reaction showed almost zero percent CO selectivity while the plasma only reaction could not show such results. Also, Pd/Al_2O_3 catalyst showed expected synergistic effect with DBD plasma. More results about these hybrid systems are shown below at Table 4. In the palladium-based catalysts reaction, catalyst that had high catalytic property also showed higher methane conversion when combined with DBD plasma.

Table 5 Reaction results of plasma-catalyst hybrid reaction

Catalyst	Input voltage(V_{p-p}) (specific input energy(J/L))	Light-off temperature(℃)		
		T_{10}	T_{50}	T_{90}
Pd/SiO_2	-	188	232	274
	2 (8-15)	63	223	274
	3 (30-51)	-	148	264
	4 (81-87)	-	40	193
$Pd/Ce_{0.7}Zr_{0.3}O_2$	-	193	251	291
	2 (12-16)	32	243	285
	3 (32-50)	-	166	275
	4 (58-91)	-	58	230
Pd/TiO_2	-	235	284	332
	2 (13-18)	45	271	330
	3 (45-68)	-	179	308
	4 (94-152)	-	70	230
Pd/CeO_2	-	184	236	276
	2 (10-19)	117	250	288
	3 (17-47)	-	217	282
	4 (102-157)	-	102	250
$Pd/\gamma-Al_2O_3$	-	191	228	274
	2 (9-14)	-	211	273
	3 (33-58)	-	115	226
	4 (95-128)	-	-	150

Chapter 4. Conclusions

In this research, to lower the light-off temperature of the methane that had stable structure, the methane complete oxidation over various palladium-based catalysts was investigated as the functions of temperature and input voltage that could influence the energy deposition in the plasma-catalyst hybrid reaction system. In the hybrid system at $2kV_{p-p}$, the methane conversion rose about 10-15% at low temperature. After a temperature reached the light-off temperature of the catalyst, the methane conversion difference between catalyst only system and hybrid system became narrow. At last, the catalyst only reaction and hybrid reaction ended at almost same reaction. At $3kV_{p-p}$, as the catalyst effect became weak and the plasma effect became strong, the slope variation was hard to be observed. Finally, at $4kV_{p-p}$, the catalyst effect almost disappeared. Thus, to observe the synergistic effect of plasma-catalyst hybridization and to save the electrical energy, proper condition of plasma source was required. Some catalysts showed higher conversion than plasma only reaction and the others were not, but all hybrid reactions showed much better CO_2 selectivity than plasma only reaction,

Despite of such advantages, more studies are necessary to use these hybrid systems in real life because when the balance gas is changed to other non-noble gases such as nitrogen, the gases will be decomposed by DBD plasma and may

produce various byproducts. In addition, the use of electrical energy during the hybrid reaction should be considered for the better energy efficiency.

References

1. Gélin, P. and M. Primet, *Complete oxidation of methane at low temperature over noble metal based catalysts: a review.* Applied Catalysis B: Environmental, 2002. **39**(1): p. 1-37.
2. Wang, Z. and A. Krupnick, *A Retrospective Review of Shale Gas Development in the United States: What Led to the Boom?* 2013.
3. Cullis, C. and B. Willatt, *Oxidation of methane over supported precious metal catalysts.* Journal of Catalysis, 1983. **83**(2): p. 267-285.
4. Muto, K.-i., N. Katada, and M. Niwa, *Complete oxidation of methane on supported palladium catalyst: Support effect.* Applied Catalysis A: General, 1996. **134**(2): p. 203-215.
5. Ribeiro, F., M. Chow, and R. Dallabetta, *Kinetics of the complete oxidation of methane over supported palladium catalysts.* Journal of Catalysis, 1994. **146**(2): p. 537-544.
6. Bozo, C., N. Guilhaume, and J.-M. Herrmann, *Role of the ceria-zirconia support in the reactivity of platinum and palladium catalysts for methane total oxidation under lean conditions.* Journal of Catalysis, 2001. **203**(2): p. 393-406.
7. Ferri, D. and L. Forni, *Methane combustion on some perovskite-like mixed oxides.* Applied Catalysis B: Environmental, 1998. **16**(2): p. 119-126.
8. Guilhaume, N. and M. Primet, *Catalytic combustion of methane: copper oxide supported on high-specific-area spinels synthesized by a sol-gel process.* Journal of the Chemical Society, Faraday Transactions, 1994. **90**(11): p. 1541-1545.
9. Ciambelli, P., et al., *La, Ca and Fe oxide perovskites: preparation, characterization and catalytic properties for methane combustion.* Applied Catalysis B: Environmental, 2001. **33**(3): p. 193-203.
10. Civera, A., et al., *Combustion synthesis of perovskite-*

type catalysts for natural gas combustion. Catalysis Today, 2003. **83**(1): p. 199-211.
11. Arai, H., et al., *Catalytic combustion of methane over various perovskite-type oxides.* Applied catalysis, 1986. **26**: p. 265-276.
12. Kim, H.H., *Nonthermal Plasma Processing for Air-Pollution Control: A Historical Review, Current Issues, and Future Prospects.* Plasma Processes and Polymers, 2004. **1**(2): p. 91-110.
13. Nozaki, T. and K. Okazaki, *Non-thermal plasma catalysis of methane: Principles, energy efficiency, and applications.* Catalysis Today, 2013.
14. Lee, D.H., et al., *Comparative Study of Methane Activation Process by Different Plasma Sources.* Plasma Chemistry and Plasma Processing, 2013: p. 1-15.
15. Da Costa, P., R. Marques, and S. Da Costa, *Plasma catalytic oxidation of methane on alumina-supported noble metal catalysts.* Applied Catalysis B: Environmental, 2008. **84**(1): p. 214-222.
16. Oda, T., *Non-thermal plasma processing for environmental protection: decomposition of dilute VOCs in air.* Journal of Electrostatics, 2003. **57**(3): p. 293-311.
17. Kogelschatz, U., *Dielectric-barrier discharges: their history, discharge physics, and industrial applications.* Plasma chemistry and plasma processing, 2003. **23**(1): p. 1-46.
18. Kraus, M., et al., *CO2 reforming of methane by the combination of dielectric-barrier discharges and catalysis.* Physical Chemistry Chemical Physics, 2001. **3**(3): p. 294-300.
19. Hammer, T., T. Kappes, and M. Baldauf, *Plasma catalytic hybrid processes: gas discharge initiation and plasma activation of catalytic processes.* Catalysis Today, 2004. **89**(1): p. 5-14.
20. Kang, W.S., et al., *Combination of Plasma with a Honeycomb-Structured Catalyst for Automobile Exhaust Treatment.* Environmental science & technology, 2013. **47**(19): p. 11358-11362.
21. Marques, R., S. Da Costa, and P. Da Costa, *Plasma-assisted catalytic oxidation of methane: On the influence*

of plasma energy deposition and feed composition. Applied Catalysis B: Environmental, 2008. **82**(1): p. 50-57.
22. Nozaki, T., et al., *Dissociation of vibrationally excited methane on Ni catalyst: Part 1. Application to methane steam reforming.* Catalysis today, 2004. **89**(1): p. 57-65.
23. Jo, S., et al., *Effect of the Electric Conductivity of a Catalyst on Methane Activation in a Dielectric Barrier Discharge Reactor.* Plasma Chemistry and Plasma Processing: p. 1-12.
24. Amouroux, J., S. Cavadias, and A. Doubla. *Carbon Dioxide reduction by non-equilibrium electrocatalysis plasma reactor*. in *IOP Conference Series: Materials Science and Engineering*. 2011. IOP Publishing.
25. Kim, T., et al., *Synergetic mechanism of methanol-steam reforming reaction in a catalytic reactor with electric discharges.* Applied Energy, 2014. **113**: p. 1692-1699.
26. Van Durme, J., et al., *Combining non-thermal plasma with heterogeneous catalysis in waste gas treatment: A review.* Applied Catalysis B: Environmental, 2008. **78**(3): p. 324-333.
27. Wang, X., et al., *Dielectric Barrier Discharge Characteristics of Multineedle-to-Cylinder Configuration.* Energies, 2011. **4**(12): p. 2133-2150.
28. Kriegseis, J., et al., *Capacitance and power consumption quantification of dielectric barrier discharge (DBD) plasma actuators.* Journal of Electrostatics, 2011. **69**(4): p. 302-312.
29. Takaki, K., et al., *Influence of electrode configuration on ozone synthesis and microdischarge property in dielectric barrier discharge reactor.* Vacuum, 2008. **83**(1): p. 128-132.
30. Zhang, Y.-p., et al., *Plasma methane conversion in the presence of carbon dioxide using dielectric-barrier discharges.* Fuel processing technology, 2003. **83**(1): p. 101-109.
31. Jiang, T., et al., *Plasma methane conversion using dielectric-barrier discharges with zeolite A.* Catalysis Today, 2002. **72**(3): p. 229-235.
32. Kolb, T., J.H. Voigt, and K.-H. Gericke, *Conversion of*

Methane and Carbon Dioxide in a DBD Reactor: Influence of Oxygen. Plasma Chemistry and Plasma Processing, 2013: p. 1-16.
33. Lee, D.H. and T. Kim, *Plasma-catalyst hybrid methanol-steam reforming for hydrogen production.* International Journal of Hydrogen Energy, 2013.
34. Tu, X. and J. Whitehead, *Plasma-catalytic dry reforming of methane in an atmospheric dielectric barrier discharge: Understanding the synergistic effect at low temperature.* Applied Catalysis B: Environmental, 2012. **125**: p. 439-448.
35. Heintze, M. and B. Pietruszka, *Plasma catalytic conversion of methane into syngas: the combined effect of discharge activation and catalysis.* Catalysis today, 2004. **89**(1): p. 21-25.
36. Jeong, J.G., et al., *Toluene Decomposition by DBD-Type Plasma Combined with Metal Oxide Catalysts Supported on Ferroelectric Materials.* Journal of Nanoscience and Nanotechnology, 2013. **13**(6): p. 4146-4149.
37. Guo, Y.-f., et al., *Toluene removal by a DBD-type plasma combined with metal oxides catalysts supported by nickel foam.* Catalysis today, 2007. **126**(3): p. 328-337.

초 록

지구온난화 가스의 한 종류로서, 메탄은 지구온난화의 주요한 원인으로 여겨지고 있다. 메탄의 안정한 C-H 결합을 저온(500℃ 이하)에서 완전히 산화시키려면 많은 양의 귀금속이 필요하다. 따라서, 이 논문에서는 촉매와 플라즈마의 하이브리드 반응을 도입하여 메탄의 발화온도를 낮추고자 하였다. 일반적인 촉매 반응에서는 반응을 일으키기 위해서 활성화 에너지만큼의 에너지가 필요하다. 따라서, 이 실험은 플라즈마가 활성 라디칼들을 생성하여, 촉매 반응의 활성화 에너지를 낮춰주는 데 도움을 줄 수 있을 것이다라는 생각에서 시작되었다. 플라즈마 소스는 크게 두 종류로 나눌 수 있다. 하나는 열 플라즈마, 다른 하나는 저온 플라즈마이다. 열 플라즈마는 촉매층의 온도를 크게 상승시켜 플라즈마-촉매 하이브리드 반응을 관찰하는 데에 방해가 될 수 있기 때문에 저온 플라즈마, 특히 유전체 장벽 방전(DBD) 플라즈마가 사용되었다. 따라서, 메탄의 완전산화 반응은 DBD 쿼츠 튜브 반응기에서 진행되었다. 이 시스템에서는, 촉매와 플라즈마가 하나의 시스템에 혼합되어 존재하였다. 현재까지 팔라듐이 담지된 촉매들이 메탄산화 반응에서 가장 높은 반응성을 보였기 때문에, 메탄 산화촉매는 Pd/Al_2O_3, Pd/CeO_2, $Pd/Ce_{0.7}Zr_{0.3}O_2$, Pd/SiO_2, Pd/TiO_2 와 같은 팔라듐이 담지된 촉매들이 사용되었다. 촉매 효과와 플라즈마 효과를 따로 관찰하기 위해서 플라즈마의 파형이나 주파수 같은 플라즈마 조건은 고정시킨 채로 플라즈마가 있을 때와 없을 때로 실험을 나누어 진행하였다. 이 때, 어떠한 입력 전압(혹은 입력 에너지)이 플라즈마-촉매 상호작용에 가장 좋은 환경을 제공하는지 관찰하기 위해, 플라즈마 조건 중 입력 전압은 $2kV_{p-p}$에서 $5kV_{p-p}$로 변화를 주었다. 또한,

플라즈마 효과를 측정하기 위해, V-Q Lissajous figure 방법을 이용하여 플라즈마 전력이 측정되었다. 촉매 없이 플라즈마만으로 반응을 진행하자, 메탄은 상온에서부터 활성화되기 시작하였다. 또한, 온도가 증가함에 따라 유전체인 쿼츠 튜브 반응기의 유전율이 달라졌기 때문에 메탄의 전환율도 증가하였다. 이 반응에서는 이산화탄소뿐만 아니라 일산화탄소도 생성되었다. 입력 전압이 $2kV_{p-p}$에서 $4kV_{p-p}$까지 변화하자, 입력 에너지의 상승으로 인해 메탄 전환율 역시 가파르게 상승하였다. 촉매반응에서는, 모든 반응에서, 200℃가 넘어가자 메탄이 활성화되기 시작하였다. 하지만 플라즈마-촉매 하이브리드 반응에서는 메탄이 상온에서부터 활성화되기 시작하였고, 생성되어서는 안 되는 일산화탄소의 선택도는 0%를 유지하였다. 이러한 결과는 촉매만의 반응에서나 플라즈마만의 반응에서는 얻어낼 수 없는 결과였다. 입력 전압의 높아지자, 플라즈마의 영향력은 강해지고, 촉매의 영향력은 줄어들어, 촉매반응의 특성을 찾기 힘들어졌다. $2kV_{p-p}$와 같이 낮은 입력 전압에서, 플라즈마-촉매 하이브리드 반응은 촉매의 반응종결 온도를 앞당기지는 못하였지만, 상온에서의 메탄 활성화와 높은 입력 전압에서는 볼 수 없는 각각의 촉매 반응의 특성을 모두 보여주었다. 또한, Pd/Al_2O_3 촉매의 경우에는 모든 입력 전압 범위에서, 플라즈마 반응에서의 메탄 전환율보다 높은 메탄 전환율을 보여주었다. 에너지 효율의 측면에서는, 낮은 입력 에너지를 사용하여 상온에서 메탄을 활성화시키고 산화 반응의 전환율을 증가시킬 수 있다는 것을 확인하였다.

주요어 : 메탄 산화, 촉매-플라즈마 하이브리드 반응, 팔라듐, 유전체 장벽 방전

학 번 : 2012-20970

감사의 글

포항을 떠나와 서울대학교에 입학했을 때가 엊그제 같은데 벌써 졸업이라니 시간이 정말 빨리 지나간 것 같습니다. 제가 이렇게 무사히 대학원 석사과정 생활을 마치고 졸업을 할 수 있기까지는 많은 분들의 도움과 가르침이 있었습니다. 이 글을 통해, 조금이나마 감사와 고마움의 말씀을 전해드리고 싶습니다.

먼저, 부족한 점이 많은 저에게 학문적 지식과 함께 삶의 지혜를 가르쳐 주신 김도희 교수님께 고개 숙여 깊은 감사의 말씀을 드리고 싶습니다. 또한, 바쁘신 와중에도 불구하고, 논문심사를 해주신 송인규 교수님과 김대형 교수님께도 진심으로 감사드립니다.

대학원 석사과정 생활 동안, 선배님들과 후배님들의 아낌없는 조언과 격려가 있어 오늘의 제가 있을 수 있을 수 있었습니다. 이 기회를 빌어, 많은 시간을 함께하였고, 또 앞으로 또 더 많은 시간을 함께 보내게 될, 연구실의 큰 형 원진이 형을 포함하여 은 누나, 소연이 누나, 승희 누나, 영석이 형, 충현이 형, 태환이 형, 종현이 모두에게 정말 감사하다는 말을 전하고 싶습니다. 그리고 연구를 진행하는 데 있어서 큰 도움을 주신, 한국기계연구원의 이대훈 박사님, 조성권 박사님, 한국화학연구원의 박용기 박사님, 최원춘 박사님, 우형이 형님께도 진심으로 감사의 말씀드립니다.

마지막으로 항상 저를 믿고 지켜봐주시는 사랑하는 부모님과 동생, 그리고 저의 소중한 친구들에게 깊이 감사드립니다. 이 분들의 믿음과 기다림, 그리고 지원이 있었기에 제가 여기까지 올 수 있었습니다. 앞으로도 기대에 보답하여 사회에 꼭 필요한 사람이 되도록 노력하겠습니다. 부모님 사랑합니다.